MULTI-PARAMETER RISK OF EASTERN REGION OF BANGLADESH DUE TO AUGUST 2024 FLOOD

Salah Uddin Ahmed Dipu*[1], M. Shahjahan Mondal[2], Faysal Bhuiyan[3], Md. Aminul Haque Laskor[4]

[1]Institute of Water and Flood Management (IWFM), Bangladesh University of Engineering and Technology (BUET), Dhaka-1000, Bangladesh, e-mail: salahuddinahmeddipu42@gmail.com
[2]Institute of Water and Flood Management (IWFM), Bangladesh University of Engineering and Technology (BUET), Dhaka-1000, Bangladesh, e-mail: mshahjahanmondal@iwfm.buet.ac.bd
[3]Institute of Water and Flood Management (IWFM), Bangladesh University of Engineering and Technology (BUET), Dhaka-1000, Bangladesh, e-mail: faysalbhuiyan001@gmail.com
[4]Institute of Water and Flood Management (IWFM), Bangladesh University of Engineering and Technology (BUET), Dhaka-1000, Bangladesh, e-mail: ahl.aminlaskor@gmail.com

***Corresponding Author**

ABSTRACT

Floods are among the most devastating natural hazards in Bangladesh, frequently impacting lives, infrastructure, and livelihoods. The eastern region of Bangladesh was severely affected by the August 2024 flood, underscoring its high susceptibility to recurrent flood disasters, due to the region's geographical setting and complex river networks. This study presents a multi-parameter flood risk assessment by integrating flood hazard and flood vulnerability indices to generate a spatial flood risk map across 11 districts in eastern Bangladesh. The flood hazard index was developed by combining the average flood depth, estimated using the Floodwater Depth Estimation Tool (FwDET v2.0), and the flood duration, derived from multi-date remote sensing images in Google Earth Engine (GEE). Data on the people affected, people displaced, and the percentage of area flooded were gathered and combined through the Analytic Hierarchy Process to develop the flood vulnerability index. A risk matrix was constructed to classify the 11 districts into five risk zones ranging from very low to very high. Feni and Noakhali districts fall under the very high-risk zone driven by high vulnerability and moderate hazard indices. Moulvibazar and Brahmanbaria are classified as the high-risk zone due to their high hazard index. Brahmanbaria recorded the longest flood duration of 10 days with an average flood depth of 2.41 m, while Moulvibazar experienced an average depth of 2.37 m and a duration of 7 days. Despite having the largest flooded area of 37.86%, Sylhet recorded the lowest number of people affected and displaced, resulting in very low flood vulnerability. Similarly, Chattogram, Khagrachari, and Cox's Bazar remained in the very low-risk zone due to their hilly topography and natural drainage systems, which collectively reduce both flood vulnerability and flood hazard indices. This integrated flood risk map can help policymakers to prioritize high-risk areas and take actions to enhance flood preparedness in the eastern region of Bangladesh.

Keywords: *risk mapping, flood hazard index, flood vulnerability index, FwDET, remote sensing*

1. INTRODUCTION

Bangladesh, a South Asian country with a monsoon climate, is highly susceptible to recurrent and intense floods, resulting in significant annual losses to human lives, the economy, and the environment (Yu et al., 2022). Between 2000 and 2019, floods affected over 1.65 billion people globally, making them the most frequent disaster type during that period (UNDRR, 2021). Bangladesh's geographic location in the Ganges-Brahmaputra-Meghna basin, combined with extensive low-lying areas and substantial monsoon precipitation, contributes to its high exposure to recurring and intensifying flood events. Each year, about 20.5% of Bangladesh is flooded on average, but during severe floods, water can cover up to 70% of the country (Islam et al., 2022). The monsoon season, which spans from June to September, brings heavy rainfall and large volumes of upstream river discharge from neighboring countries, often leading to widespread riverine flooding (Dewan, 2015). These monsoon floods pose significant risks to human lives, agriculture, infrastructure, and overall economic development (Parvez et al., 2022; Zayed et al., 2024).

With the growing frequency and the severity of flood events, particularly in climate-vulnerable countries like Bangladesh, flood risk assessment is essential for developing effective flood mitigation and management strategies. Flood risk is typically conceptualized as a function of hazard index and vulnerability index (Prall et al., 2024; Tabasi et al., 2025). The hazard index is an indicator used to evaluate the severity of a potentially damaging event, whether natural or human-induced, within a defined geographic area (Prall et al., 2024). In the context of floods, this index incorporates parameters such as flood depth, duration, and velocity, which are often derived using hydrologic models or remote sensing tools (Parsian et al., 2021; Tingsanchali & Promping, 2022). In contrast, the vulnerability index refers to the degree to which a system or population is likely to suffer damage and is influenced by socio-economic, demographic, and infrastructural factors (Forbes-Mewett & Nguyen-Trung, 2019). Nowadays, remote sensing is widely used in flood mapping due to its ability to accurately capture flood extent through high-resolution imagery, a range of spectral bands, varying sensor incidence angles, and multiple polarization modes (Prall et al., 2024). Remote sensing offers a cost-effective and efficient method for flood hazard mapping due to its ability to capture frequent, high-resolution observations of the Earth's surface (Amitrano et al., 2024). Satellites like Sentinel-1, RISAT-1, and Radarsat-2 provide valuable data for tracking flood extent, duration, and trends over time (Prall et al., 2024). The use of Synthetic Aperture Radar (SAR) data from platforms such as Sentinel-1 enables rapid and reliable detection of flood extent, regardless of cloud cover and solar illumination (Zhao et al., 2024).

In August 2024, a severe flash flood hit 11 districts in Eastern Bangladesh, affecting 5.8 million (NDRCC), residents and displacing over 0.5 million people (National Disaster Response Coordination Center 2024; Needs Assessment Working Group Bangladesh, 2024). This study presents a flood risk map for the eastern region affected by the August 2024 flood by integrating vulnerability and hazard indices. The vulnerability index is derived from three key indicators—the number of people affected, the number of people displaced, and the area flooded—using data from both remote sensing and official damage assessments. These indicators are weighted using the multi-criteria decision-making (MCDM) method, such as the Analytic Hierarchy Process (AHP), to construct a Flood Vulnerability Index (FVI) (Hoque et al., 2019; Saaty & Kearns, 1985). Flood depth was estimated using the Flood Water Depth Estimation Tool (FwDET v2.0) along with Sentinel-1 SAR-derived flood extent data (Cohen et al., 2019). Flood duration was determined by processing and analyzing multi-date Sentinel-1 images, in Google Earth Engine (GEE) (Rättich et al., 2020). These parameters were then combined using AHP to create the Flood Hazard Index (FHI). The FHI and FVI are subsequently combined to compute a Flood Risk Index, which is then mapped across the 11 districts to classify them into different risk zones. The resulting flood risk map provides essential insights for disaster response, early warning system design, and long-term adaptation planning.

2. METHODOLOGY

2.1 Study area

In August 2024, Eastern Bangladesh was severely affected by widespread flooding, driven by the combined effects of heavy monsoonal precipitation and upstream inflows from transboundary rivers. Figure 1 shows the 11 selected districts in Eastern Bangladesh, which include Sylhet, Moulvibazar, Habiganj, Brahmanbaria, Cumilla, Feni, Noakhali, Lakshmipur, Chattogram, Khagrachhari, and Cox's Bazar, while Table 1 presents the data types and sources used in the study.

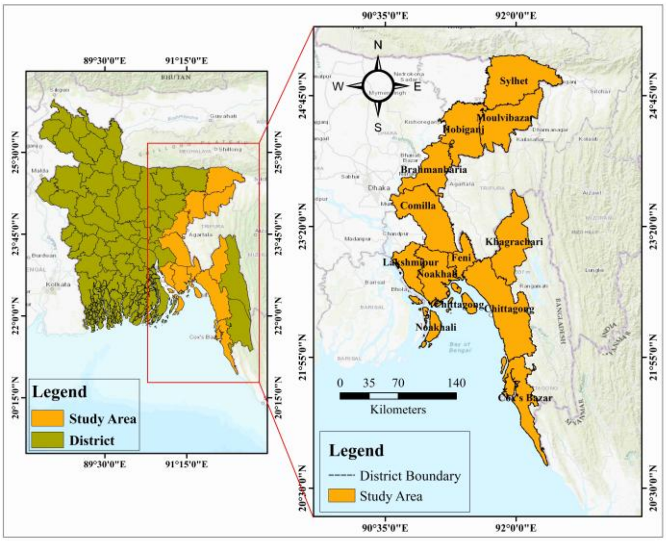

Figure 1: Location of the study area

Table 1: Data types and sources used in the present study

Data type	Data source	Time Period	Relevance
DEM	USGS/SRTMGL1_003	2024	Used in FwDET
Flood depth	FwDET v2.0 (Cohen et al., 2019)	Aug. 2024	Input for FHI
Flood duration	Copernicus Browser	Aug.-Sep. 2024	Input for FVI
Population and district area	Bangladesh Bureau of Statistics (BBS)	2022	Used to calculate PA (%), PD (%) and AF (%)
People affected and displaced	National Disaster Response Coordination Center (NDRCC) & Needs Assessment Working Group Bangladesh	Aug. 2024	Input for FHI
Area flooded	Sentinel-1 SAR data	Aug. 2024	Input for FHI & FVI
Expert judgment (AHP weights)	10 Questionnaire survey (3 faculty members from BUET, SUST, JU, 5 government officers from BIWTA, BWDB, DDM and 2 NGO personnel from WSUP, O. Creeds,)	2025	Used to determine weights
Water level	BWDB	2024	Used for validation
Rainfall	BMD	1983-2024	Used for climatic anomaly

2.2 Assessment of FHI

2.2.1 Flood depth

The FHI is usually calculated using three parameters: flood depth, flood duration, and flow velocity. However, in this study, the hazard index was derived using only two key parameters: flood depth and flood duration. Flood depth was estimated using a remote sensing-based geospatial method implemented in Google Earth Engine, based on the conceptual framework of the Flood Water Depth Estimation Tool (FwDET v2.0) (Cohen et al., 2018). The calculation utilized three primary inputs: a binary flood extent mask (0 = non-flooded area, 1 = flooded area), a permanent water body, and a digital elevation model (DEM) from the SRTM 30-meter resolution DEM from USGS. Binary flood extent maps are generated from Sentinel-1 data by analyzing the backscatter differences between flooded and non-flooded areas using SAR images; for the August 2024 flood, the flood extent map was created by analyzing images from 01/08/2024 to 31/09/2024.

Permanent water masks were created using multi-temporal SAR images. Water was identified through an improved multi-index approach combining the Normalized Difference Water Index (NDWI), the Modified Normalized Difference Water Index (MNDWI), the Normalized Difference Vegetation Index (NDVI), and the Enhanced Vegetation Index (EVI). A pixel was classified as water if NDWI > -0.1 and (MNDWI > NDVI or MNDWI > EVI), effectively separating water from vegetation, built-up areas, and shadows (Wang et al., 2023). Water masks were generated for all images, and a water frequency (WF) map was created by calculating the percentage of time each pixel was classified as water. Pixels with 95% < WF ≤ 100% were classified as permanent water bodies, representing areas consistently inundated throughout the study period. Equation (1) was used to calculate WF:

$$WF = \frac{\sum_{t=1}^{N}(\varepsilon t=1)}{N} \times 100\% \quad (1)$$

Where ε represents the corresponding cell value of the i_{th} open-surface water body map (1 for water, 0 for non-water), accumulated in GEE with ‘sum’, where N denotes the total number of valid observations of Sentinel-1 image elements in a given period (Wang et al., 2023). DEM outliers were filtered using a modified Z-score and local median smoothing to improve accuracy. The flood depth was then derived by subtracting the smoothed DEM from the estimated water surface elevation. Flood depth is categorized into five classes: D_0 < 0.3 m, D_1 (0.3-0.9 m), D_2 (0.9-1.8 m), D_3 (1.8-3 m), and D_4 > 3 m (Akhter et al., 2025). Finally, average flood depth was calculated for 11 districts. This tool rapidly estimates flood depth using only a binary flood extent map and a DEM, without requiring hydraulic data, making it ideal for emergency response and large-scale flood hazard assessment (Cohen et al., 2019).

The average flood depth was converted to a normalized scale ranging from 1 to 100. Normalization is a data pretreatment technique used to eliminate differences in the units and scales of various parameters by converting them into a common, unitless scale. For normalization, the following equation (2) (Chyon et al., 2023) was used:

$$Normalization\ Score = 1 + \frac{(100-1) \times (Actual\ value - Minimum\ Value)}{Maximum\ value - Minimum\ value} \quad (2)$$

2.2.2 Flood duration

Flood duration estimation was performed through a time-series analysis of binary flood extent maps, using flood extent masks derived from Sentinel-1 data to create a spatially explicit map that indicates the duration of flooding for each pixel within a defined time range. During the preprocessing phase, all input datasets were harmonized to ensure consistency in coordinate reference system, spatial extent, and resolution. Once preprocessed, the flood and valid masks were stacked along the temporal axis, with the most recent acquisition date placed on the right. This temporal stack served as input for a time-series analysis, during which the start and end dates of each flood event, as well as any observation gaps, were identified for every pixel, ultimately leading to the Total Flood Duration (TFD). TFD is computed for each pixel within a defined time period, from 01/08/2024 to 31/09/2024. Figure 2 shows a schematic illustration of the approach that was applied to compute the TFD of a single pixel over a period of 10 days (D1–D10). The blue boxes mark dates when the pixel was identified as being flooded. The white boxes represent days without an observation at a particular pixel location; this may be due to either the pixel being marked as invalid or because there was a lack of available satellite imagery on the given day.

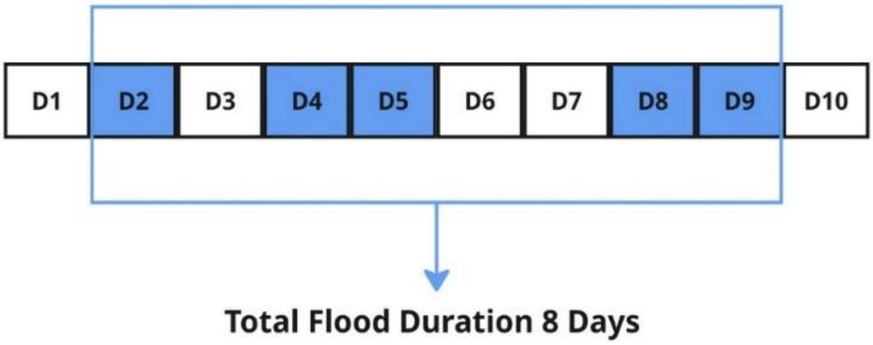

Figure 2: Total flood duration

The duration of a flood can be computed, in days, between its start and end date. Therefore, Total Flood Duration (TFD) is defined as the sum of the durations of all flood periods within a given time period and can be calculated for a single pixel i as the following equation (3) (Rättich et al., 2020):

$$TFD_i = \sum_{f=1,n} D_{f,end} - D_{f,start} \tag{3}$$

TFD was converted to the average flood duration for 11 districts and subsequently normalized using Equation (2). The final FHI value was categorized into five zones: 0–20 for very low, 21–40 for low, 41–60 for moderate, 61–80 for high, and 81–100 for very high hazard zone.

2.3 Assessment of FVI

Flood vulnerability refers to the degree to which a community or region is susceptible to harm from flooding, based on a combination of social and physical exposure indicators (Lee & Choi, 2019). The following equation (4) was used to calculate the flood vulnerability index (FVI):

$$FVI = \alpha\, PA\,(\%) + \beta\, PD\,(\%) + \gamma\, AF\,(\%) \tag{4}$$

Where PA is the number of people affected, PD is the number of people displaced, and AF is the area flooded. These three parameters were selected based on their association with different impact categories: PA for human impacts, PD for social impacts, and AF for economic impacts. AF was derived from the inundation map generated using the remote sensing platform in Google Earth Engine, where permanent water bodies were masked to isolate flood-affected areas. To detect the AF, Sentinel-1 SAR data (VV polarization, ascending orbit, IW mode) were used due to their cloud-penetrating capability, which is especially valuable during the monsoon season (Amitrano et al., 2024). A median composite image was generated for the flood period. A threshold-based classification was applied to the Sentinel-1 VV band. A backscatter threshold of –13 dB was empirically set to differentiate between flooded and non-flooded areas, based on known radar responses to open water surfaces. Pixels with backscatter values below this threshold were classified as flooded, while others were marked as non-flooded or no data (Arora et al., 2025). PA (%), PD (%), and AF (%) are then normalized using equation (2) and multiplied by their respective weights to calculate the final FVI. The FVI value was categorized into five zones: 0–20 for very low, 21–40 for low, 41–60 for moderate, 61–80 for high, and 81–100 for very high vulnerability zone.

2.4 Assessment of flood risk

Flood risk can be assessed using a variety of conceptual and quantitative methods, depending on the purpose and scale of analysis. One common method defines risk as the product of probability and consequences, where probability refers to the likelihood of a hazardous event, and consequences represent the resulting damage or loss. A widely accepted framework given by the IPCC in its Sixth Assessment Report (IPCC, 2022) conceptualizes risk as a function of hazard, vulnerability, and exposure. This framework has been applied extensively in flood risk studies, as it captures both the physical characteristics of flood events and the socio-economic conditions of exposed populations and assets (Chyon et al., 2023; Khan et al., 2025). Some studies simplify this further by defining risk as a function of only hazard and vulnerability, especially in contexts where detailed exposure data are lacking or vulnerability includes exposure (Hazarika et al., 2018). In this study the following risk equation (5) (Hazarika et al., 2018) was used for 11 districts:

$$\textit{Flood Risk} = \textit{Flood Hazard Index} \times \textit{Flood Vulnerability Index} \tag{5}$$

3. RESULTS & DISCUSSION

3.1 FHI

3.1.1 Flood depth

The flood depth derived from FwDET was validated using water level data from 5 BWDB stations. The average flood depth at each station was calculated by subtracting the average ground elevation from the peak water level. These values were compared with FwDET-derived depths, as shown in Table 2. The validation showed that FwDET closely matched observed depths but overestimated flood depth in some areas. Validation could not be performed for other districts, as the stations were outside the flooded area.

Table 2: Average flood depth validation with BWDB station data

District	River Name	Station Name and ID	Max. WL (mMSL)	Avg. Flood Depth (m)	Avg. Flood Depth from FwDET(m)
Sylhet	Surma-Meghna	Sylhet-SW267	13.60	1.98	2.21
Moulvibazar	Manu	Moulvibazar-SW202	12.49	2.26	2.37
Habiganj	Khowai	Habiganj-SW159	11.00	2.55	2.42
Cumilla	Gumti	Debidwar-Sw114	8.77	1.67	1.74
Feni	Muhuri	Parshuram-SW212	14.19	1.98	2.09
Chattogram	Halda	Narayanhat-SW117	16.17	1.39	1.19

The average flood depth shown in Figure 3 varies significantly across districts, reflecting the differing impacts of flooding. Habiganj experiences the highest average flood depth at 2.42 m, indicating severe flooding, while Chattogram sees the lowest at 1.19 m, suggesting less impact. Other districts like Sylhet, Moulvibazar, and Brahmanbaria face considerable flooding with depths of 2.21 m, 2.37 m, and 2.41 m, respectively.

3.1.2 Flood duration

The flood duration derived from GEE was validated with the observed flood days from the 5 BWDB stations, where flood days are defined as the number of days the water level crosses the danger level, as shown in Table 3. The validation shows a close match between the observed flood days and the average flood duration derived from remote sensing. Validation could not be performed for other districts, as the stations were outside the flooded area.

Table 3: Average flood duration validation with BWDB station data

District	River Name	Station Name and ID	Observed Flood Days	Average Flood Duration from GEE (Days)
Sylhet	Surma-Meghna	Sylhet-SW267	6	7
Moulvibazar	Manu	Moulvibazar-SW202	6	7
Habiganj	Khowai	Habiganj-SW159	8	9
Cumilla	Gumti	Cummilla Sadar-SW110	7	7
Feni	Muhuri	Parshuram-SW212	6	6
Chattogram	Halda	Narayanhat-SW117	4	5

Figure 3 presents the flood duration for various districts, reflecting the length of time each district experienced flooding. Sylhet, Moulvibazar, and Cumilla each had an average flood duration of 7 days, while Habiganj experienced a slightly longer duration of 9 days. Brahmanbaria had the longest flood duration at 10 days, indicating a prolonged flooding event. Feni had an average duration of 6 days, while Noakhali had 7 days, and Lakshmipur had 8 days, indicating varied flood durations across the region.

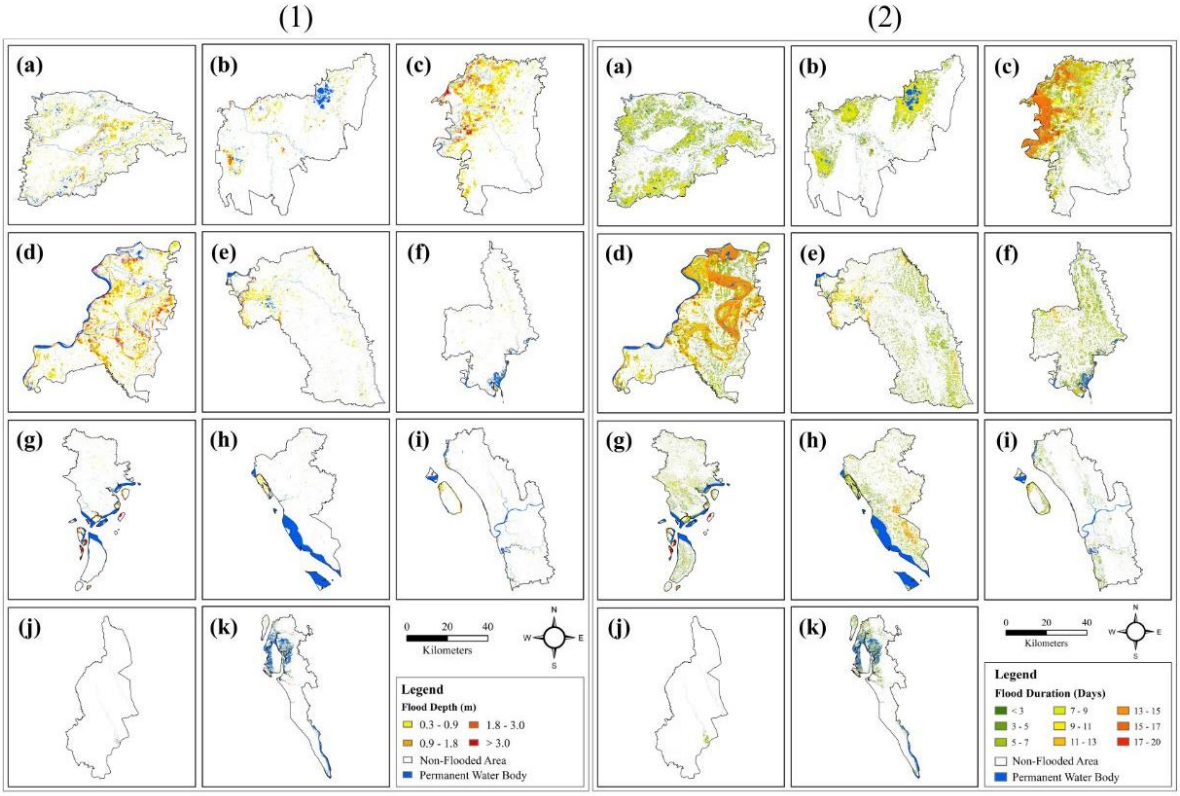

Figure 3: (1) Flood depth and (2) flood duration of 11 districts: (a) Sylhet, (b) Moulvibazar, (c) Habiganj, (d) Brahmanbaria, (e) Cumilla, (f) Feni, (g) Noakhali, (h) Lakshmipur, (i) Chattogram, (j) Khagracgari, and (k) Cox's Bazar

3.1.3 Flood hazard map

The flood hazard map shown in Figure 4 illustrates the hazard zones across 11 districts due to the August 2024 flood. Districts like Habiganj and Brahmanbaria fall within the very high hazard zone. Sylhet and Moulvibazar are classified in the high hazard zone, while districts such as Cumilla, Feni, Noakhali, and Lakshmipur fall under the moderate hazard zone. Cox's Bazar is in the low hazard zone, and Chattogram and Khagrachari are in the very-low hazard zone, with relatively lower flood severity.

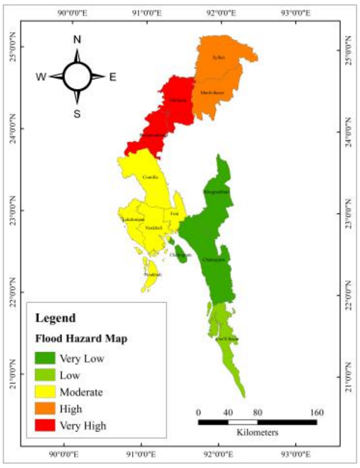

Figure 4: Flood hazard map of 11 districts due to August 2024 flood

3.2 FVI

3.2.1 People affected and displaced

Figure 5 presents the percentage of PA and PD by the flood across 11 districts in Bangladesh, highlighting significant regional variation in impact. Feni and Noakhali recorded the highest levels of impact, with 60.65% and 58.63% PA, respectively, and notable PD rates of 12.48% and 3.32%. Lakshmipur also recorded a high proportion of PA, 37.3%, and a PD rate of 3.77%. In contrast, Sylhet, Habiganj, and Brahmanbaria recorded minimal impacts, with less than 3% PA and less than 1% PD.

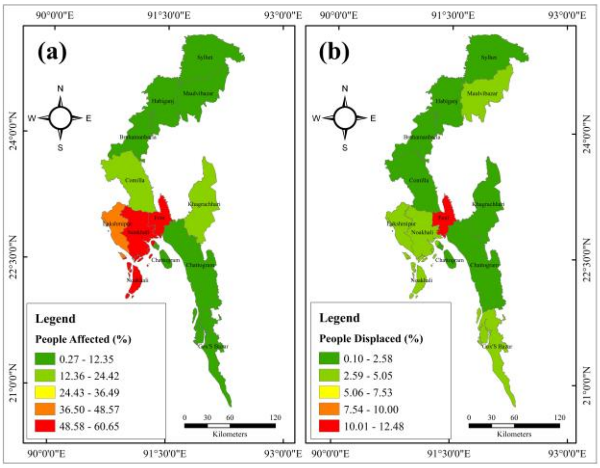

Figure 5: (a) Percent people affected and (b) percent people displaced due to August 2024 flood

3.2.2 Area flooded

Figure 6 illustrates the flooded and non-flooded areas across various districts. Sylhet experienced the highest level of flooding, with 37.86% AF, followed by Brahmanbaria and Habiganj with 37.00% and 35.18% AF, respectively, indicating significant flooding. Moulvibazar experienced a moderate impact, with 23.15% AF. Feni, Noakhali, and Lakshmipur recorded 27.29%, 24.99%, and 21.63% AF, respectively, indicating notable flooding, though less extreme than in the previously mentioned districts. Chattogram and Khagrachari experienced the least flooding, with 8.35% and 2.65% AF, respectively. Cox's Bazar experienced moderate flooding, with 12.35% AF.

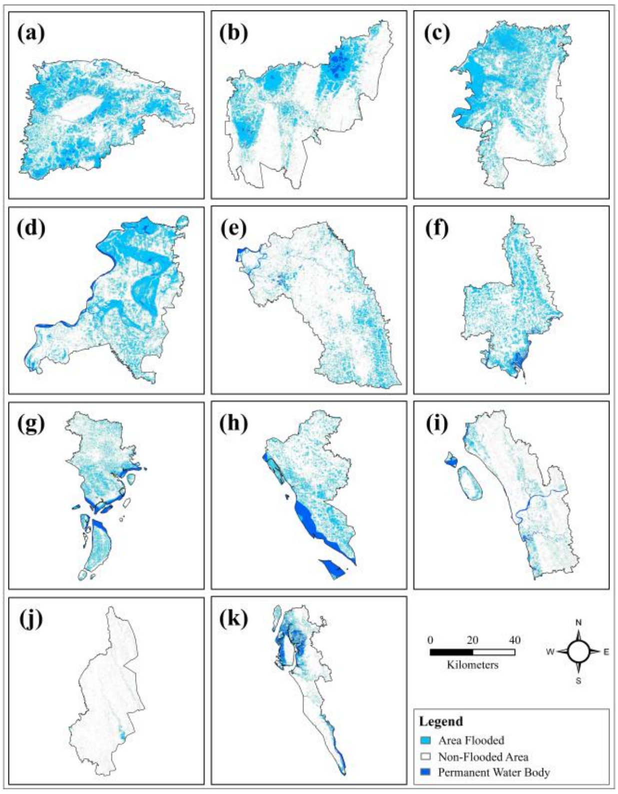

Figure 6: Area flooded and permanent water body of 11 districts: (a) Sylhet, (b) Moulvibazar, (c) Habiganj, (d) Brahmanbaria, (e) Cumilla, (f) Feni, (g) Noakhali, (h) Lakshmipur, (i) Chattogram, (j) Khagracgari, and (k) Cox's Bazar

3.2.3 Flood vulnerability map

Figure 7 illustrates the flood vulnerability map, highlighting the spatial variation in vulnerability levels across the studied districts. Most districts, such as Sylhet, Moulvibazar, Habiganj, Brahmanbaria, Cumilla, Lakshmipur, Chattogram, and Cox's Bazar, fall within the low-vulnerability zone. Khagrachari, with the lowest vulnerability, is placed in the very-low category. In contrast, Feni and Noakhali are categorized in the high vulnerability zone due to the highest PA among the 11 districts, marking them as key areas for focused adaptation and risk reduction efforts.

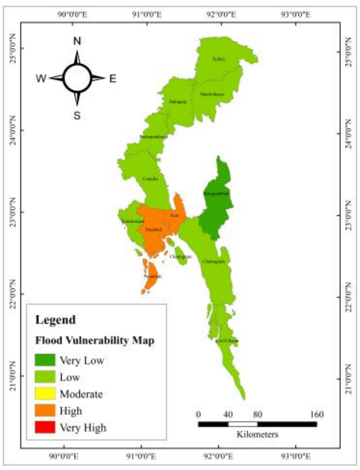

Figure 7: Flood vulnerability map of 11 districts due to August 2024 flood

3.3 Flood risk map

The final risk map shown in Figure 8 is based on the combination of the FVI and FHI. The FVI varies from very high to very low depending on the percentages of PA, PD, and AF, whereas the FHI varies according to flood severity, controlled by flood depth and flood duration. Feni and Noakhali districts emerge as the highest risk zone due to their high FVI and moderate FHI. Moulvibazar and Brahmanbaria are categorized as high-risk zone due to the very high FHI of Brahmanbaria and high FHI of Moulvibazar, despite both having moderate FVI. Habiganj and Sylhet experience high and very high FHI, respectively, but their low FVI places them in the moderate-risk zone. Lakshmipur is classified as a moderate-risk zone due to its moderate FHI and low FVI. Cumilla is considered a low-risk zone because of its moderate FHI and low FVI. Chattogram, Khagrachari, and Cox's Bazar fall into the very low-risk zone due to the very low FHI of Chattogram and Khagrachari and low FHI of Cox's Bazar, along with very low FVI of Khagrachari and low FVI of Chattogram and Cox's Bazar.

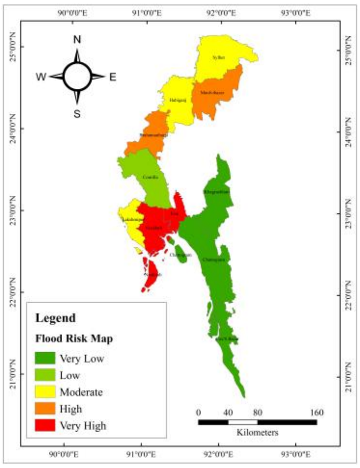

Figure 8: Flood risk map of 11 districts due to August 2024 flood

3.4 Rainfall analysis

Figure 9(a) illustrates the spatial distribution of total monsoon rainfall, with the highest rainfall in Lakshmipur, Noakhali, and Feni, and lowest rainfall in Sylhet and Moulvibazar. Figure 9(b) shows the climatic anomaly of total monsoon rainfall for 2024 relative to the 30-year mean, revealing significant positive anomalies in Lakshmipur and Noakhali and negative anomalies in Sylhet and Moulvibazar. This pattern aligns with the 2024 eastern Bangladesh flood, where heavy rainfall in low-lying coastal districts like Lakshmipur, Noakhali, and Feni contributed to extensive flooding in these areas.

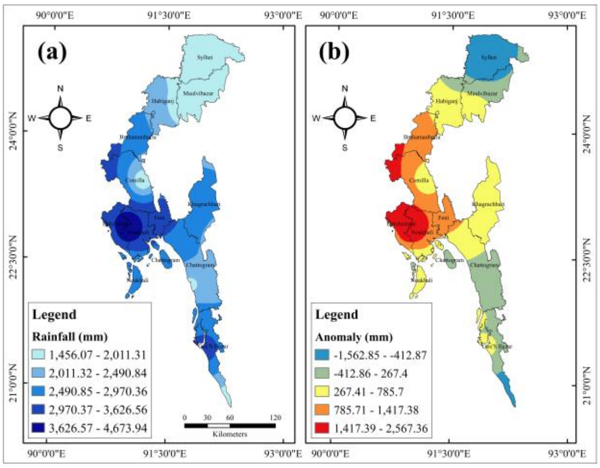

Figure 9: (a) Total monsoon rainfall in 2024, and (b) climatic anomaly for the year 2024

4. CONCLUSIONS

The flood risk assessment across 11 districts in eastern Bangladesh reveals significant variation in hazard, vulnerability, and overall risk zones. Feni and Noakhali emerged as very high-risk zone due to high vulnerability and moderate hazard, while Moulvibazar and Brahmanbaria fall under high-risk zone. Lakshmipur is classified as a moderate-risk zone. Hilly districts such as Chattogram, Khagrachari, and Cox's Bazar benefit from natural drainage due to their elevated terrain, resulting in smaller flood-affected areas and minimal displacement, and are thus classified as very low-risk zone. Analysis of monsoon rainfall shows that Lakshmipur, Noakhali, and Feni received the highest rainfall in 2024, with significant positive anomalies compared to the 30-year climatological mean, driving extensive monsoon flooding in these low-lying coastal districts. The findings of this study can assist policymakers in developing region-specific flood management strategies for high-risk districts, particularly those vulnerable to sudden and severe flooding events, such as Feni and Noakhali.

Declaration of the Use of Generative AI and AI-Assisted Technologies

During the preparation of this work, the authors used paraphrasing tools to improve the readability and language of the manuscript. After using these tools, the authors reviewed and edited the content as needed and took full responsibility for the final manuscript.

REFERENCES

Akhter, S., Rahman, M. M., & Monir, M. M. (2025). Flood susceptibility analysis to sustainable development using MCDA and support vector machine models by GIS in the selected area of the Teesta river floodplain, Bangladesh. HydroResearch, 8, 127–138. https://doi.org/10.1016/j.hydres.2024.10.004

Amitrano, D., Di Martino, G., Di Simone, A., & Imperatore, P. (2024). Flood Detection with SAR: A Review of Techniques and Datasets. Remote Sensing, 16(4). https://doi.org/10.3390/rs16040656

Arora, M., Setia, R., Singh, R., Singh, S. K., Kumar, S., & Pateriya, B. (2025). Mapping of flood inundated areas using earth observation data and cloud computing platform. Journal of Atmospheric and Solar-Terrestrial Physics, 274, 106567. https://doi.org/10.1016/J.JASTP.2025.106567

Chyon, M. S. A., Biswas, S., Mondal, M. S., Roy, B., & Rahman, A. (2023). Integrated assessment of flood risk in Arial Khan floodplain of Bangladesh under changing climate and socioeconomic conditions. Journal of Flood Risk Management, 16(2). https://doi.org/10.1111/jfr3.12876

Cohen, S., Brakenridge, G. R., Kettner, A., Bates, B., Nelson, J., McDonald, R., Huang, Y. F., Munasinghe, D., & Zhang, J. (2018). Estimating floodwater depths from flood inundation maps and topography. Journal of the American Water Resources Association, 54(4), 847–858. https://doi.org/10.1111/1752-1688.12609

Cohen, S., Raney, A., Munasinghe, D., Derek Loftis, J., Molthan, A., Bell, J., Rogers, L., Galantowicz, J., Robert Brakenridge, G., Kettner, A., Huang, Y. F., & Tsang, Y. P. (2019). The Floodwater Depth Estimation Tool (FwDET v2.0) for improved remote sensing analysis of coastal flooding. Natural Hazards and Earth System Sciences, 19(9), 2053–2065. https://doi.org/10.5194/nhess-19-2053-2019

Dewan, T. H. (2015). Societal impacts and vulnerability to floods in Bangladesh and Nepal. Weather and Climate Extremes, 7, 36–42. https://doi.org/10.1016/j.wace.2014.11.001

Forbes-Mewett, H., & Nguyen-Trung, K. (2019). Defining Vulnerability. In Vulnerability in a Mobile World (pp. 5–27). Emerald Group Publishing Ltd. https://doi.org/10.1108/978-1-78756-911-920191004

Hazarika, N., Barman, D., Das, A. K., Sarma, A. K., & Borah, S. B. (2018). Assessing and mapping flood hazard, vulnerability and risk in the Upper Brahmaputra River valley using stakeholders' knowledge and multicriteria evaluation (MCE). Journal of Flood Risk Management, 11, S700–S716. https://doi.org/10.1111/jfr3.12237

Hoque, M. A. A., Tasfia, S., Ahmed, N., & Pradhan, B. (2019). Assessing spatial flood vulnerability at Kalapara upazila in Bangladesh using an analytic hierarchy process. Sensors, 19(6). https://doi.org/10.3390/s19061302

IPCC. (2022). Climate Change 2022: Impacts, Adaptation, and Vulnerability. Contribution of Working Group II to the Sixth Assessment Report of the Intergovernmental Panel on Climate Change, ed. H.-O. Pörtner et al. Cambridge University Press, Cambridge, UK and New York, NY, USA, pp 3–33. https://www.ipcc.ch/report/ar6/wg2/

Islam, M. S., Samreth, S., Islam, A. H. M. S., & Sato, M. (2022). Climate change, climatic extremes, and households' food consumption in Bangladesh: A longitudinal data analysis. Environmental Challenges. https://doi.org/10.1016/j.envc.2022.100495

Khan, N. A., Alzahrani, H., Bai, S., Hussain, M., Tayyab, M., Ullah, S., Ullah, K., & Khalid, S. (2025). Flood risk assessment in the Swat river catchment through GIS-based multi-criteria decision analysis. Frontiers in Environmental Science, 13. https://doi.org/10.3389/fenvs.2025.1567796

Lee, J. S., & Choi, H. Il. (2019). Comparative analysis of flood vulnerability indicators by aggregation frameworks for the IPCC's assessment components to climate change. Applied Sciences, 9(11). https://doi.org/10.3390/app9112321

National Disaster Response Coordination Center (NDRCC). (2024). Inter-cluster Coordination Group-Humanitarian Task Team Bangladesh: Eastern Flash Floods 2024. Retrieved from https://response.reliefweb.int/bangladesh/needs

Needs Assessment Working Group Bangladesh. (2024). Loss and Damage of Eastern Flash Flood 2024 Analysis from D-Form. https://response.reliefweb.int/bangladesh/needs-

Parsian, S., Amani, M., Moghimi, A., Ghorbanian, A., & Mahdavi, S. (2021). Flood hazard mapping using fuzzy logic, analytical hierarchy process, and multi-source geospatial datasets. Remote Sensing, 13(23). https://doi.org/10.3390/rs13234761

Parvez, M., Islam, M. R., & Dey, N. C. (2022). Household food insecurity after the early monsoon flash flood of 2017 among wetland (Haor) communities of northeastern Bangladesh: a cross-sectional study. Food and Energy Security, 11(1). https://doi.org/10.1002/fes3.326

Prall, M. C., Brandt, U. S., Halvorsen, N. S., Hansen, M. U., Dahlberg, N., & Andersen, K. J. (2024). A comprehensive approach for assessing social flood vulnerability and social flood risk: The case of Denmark. International Journal of Disaster Risk Reduction, 111, 104686. https://doi.org/10.1016/J.IJDRR.2024.104686

Rättich, M., Martinis, S., & Wieland, M. (2020). Automatic flood duration estimation based on multi-sensor satellite data. Remote Sensing, 12(4). https://doi.org/10.3390/rs12040643

Saaty, T. L., & Kearns, K. P. (1985). The Analytic Hierarchy Process. In Analytical Planning (pp. 19–62). Elsevier. https://doi.org/10.1016/b978-0-08-032599-6.50008-8

Tabasi, N., Fereshtehpour, M., & Roghani, B. (2025). A review of flood risk assessment frameworks and the development of hierarchical structures for risk components. Discover Water, 5(1). https://doi.org/10.1007/s43832-025-00193-2

Tingsanchali, T., & Promping, T. (2022). Comprehensive Assessment of flood hazard, vulnerability, and flood risk at the household level in a municipality area: A case study of Nan Province, Thailand. Water, 14(2). https://doi.org/10.3390/w14020161

UNDRR. (2021). United Nations Office for Disaster Risk Reduction. https://www.undrr.org/

Wang, W., Teng, H., Zhao, L., & Han, L. (2023). Long-term changes in water body area dynamic and driving factors in the Middle-Lower Yangtze Plain based on multi-source remote sensing data. Remote Sensing, 15(7). https://doi.org/10.3390/rs15071816

Yu, Q., Wang, Y., & Li, N. (2022). Extreme Flood Disasters: Comprehensive impact and assessment. Water, 14(8). https://doi.org/10.3390/w14081211

Zayed, S., Morrison, L. T. R., Lapidus, D., Gallaher, M., Letterman, C., Allpress, J. L. E., & Cummings, S. (2024). Valuing the economic impact of river floods and early flood warning for Households in Bangladesh. Economics of Disasters and Climate Change. https://doi.org/10.1007/s41885-024-00156-2

Zhao, J., Xiong, Z., & Zhu, X. X. (2024). UrbanSARFloods: Sentinel-1 SLC-based benchmark dataset for urban and open-area flood mapping. http://arxiv.org/abs/2406.04111